catalysts

MDPI

Article

The Role of Ruthenium in CO_2 Capture and Catalytic Conversion to Fuel by Dual Function Materials (DFM)

Shuoxun Wang [1], Erik T. Schrunk [2], Harshit Mahajan [2] and Robert J. Farrauto [1,*]

[1] Earth and Environmental Engineering, Columbia University in the City of New York, New York 10027, NY, USA; sw2916@columbia.edu

[2] Chemical Engineering, Columbia University in the City of New York, New York 10027, NY, USA; ets2130@columbia.edu (E.T.H.); hm2655@columbia.edu (H.M.)

* Correspondence: rf2182@columbia.edu (R.J.F.); Tel.: +1-212-854-6390

Academic Editors: Albert Demonceau, Ileana Dragutan and Valerian Dragutan
Received: 7 February 2017; Accepted: 14 March 2017; Published: 17 March 2017

Abstract: Development of sustainable energy technologies and reduction of carbon dioxide in the atmosphere are the two effective strategies in dealing with current environmental issues. Herein we report a Dual Function Material (DFM) consisting of supported sodium carbonate in intimate contact with dispersed Ru as a promising catalytic solution for combining both approaches. The Ru-Na_2CO_3 DFM deposited on Al_2O_3 captures CO_2 from a flue gas and catalytically converts it to synthetic natural gas (i.e., methane) using H_2 generated from renewable sources. The Ru in the DFM, in combination with H_2, catalytically hydrogenates both adsorbed CO_2 and the bulk Na_2CO_3, forming methane. The depleted sites adsorb CO_2 through a carbonate reformation process and in addition adsorb CO_2 on its surface. This material functions well in O_2- and H_2O-containing flue gas where the favorable Ru redox property allows RuO_x, formed during flue gas exposure, to be reduced during the hydrogenation cycle. As a combined CO_2 capture and utilization scheme, this technology overcomes many of the limitations of the conventional liquid amine-based CO_2 sorbent technology.

Keywords: supported Ru and sodium carbonate; dual function material; CO_2 capture in flue gas; conversion to synthetic natural gas; redox properties of Ru

1. Introduction

As predicted by the Intergovernmental Panel on Climate Change (IPCC), carbon dioxide in the atmosphere may reach 570 ppmv by the year of 2100, accompanied by a rise in the mean global temperature of 1.9 °C and mean sea level by 38 cm [1–3]. Excess carbon dioxide emission results primarily from anthropogenic activities by fossil fuel combustion for power generation, industrial manufacturing, and transportation [4]. Due to the CO_2 accumulation and the rising demand of energy, sustainable energy development [5,6], and CO_2 capture, storage and utilization (CCSU) [7] are two efficient methods to combat green-house gas emissions and associated climate change.

For a decade, various processes and materials have been proposed for CO_2 capture, with extensive reviews available [8,9]. The aqueous amine–based sorbent technology is still the most popular and developed approach toward capturing CO_2 from flue gas. However, the sorbent regeneration for separation of CO_2 and H_2O from the amine solution by distillation is highly energy intensive. The separated CO_2 must then be transported to a recovery site for processing, which adds to the expense. Furthermore, the O_2 containing flue gas deteriorates the amine, limiting its ability to be recycled [10].

Recently, several unique material combinations and processes for upgrading CO_2 have been reported. A super-dry reforming process involving chemical looping in which CO_2 is utilized for enhancing CO production at 750 °C has been reported. Nickel catalyzes the dry reforming of CH_4

leading to a redox reaction of iron oxides. CO_2 is adsorbed on CaO/Al_2O_3, providing a series of equilibrium shifts enhancing CO production for ultimate use in synthesis gas reactions [11]. Another interesting approach for enhanced CO production combines a reduced Fe, Cr, Cu reverse water gas shift (RWGS) catalyst with K_2CO_3 as a CO_2 adsorbent. Approximately 6% CO_2 in N_2 is adsorbed on K_2CO_3 at 550 °C. At the same temperature, injected H_2 reacts with adsorbed CO_2 generating CO and H_2O via the RWGS reaction. A weakness in the process is the deterioration of performance in O_2, limiting this to O_2-free CO_2 streams [12].

Ruthenium is a well-known noble metal catalyst often used commercially for homogeneous or heterogeneous catalytic reactions requiring a high degree of product selectivity, including aromatic ring saturation to cyclo-hexyl derivatives, saturation of allyl compounds, organic acid hydrogenation to alcohols, hydrogenation of sugars [13], steam reforming of hydrocarbons for H_2 production [14], selective homogeneous catalysis for the oxidation of primary alcohols to aldehydes [15], and homogenous chiral synthesis [16]. It is also used for ammonia synthesis [17], preferential oxidation of CO in H_2 [18], Fischer-Tropsch processes [19], electrochemical chlorine evolution [20], and methanation of CO and CO_2 [21–23]. In representative reactions, such as those mentioned above, all require either the metal, its oxide, or an organo-metal complex form of Ru as the catalyst. A unique feature of Ru/RuO_x is its redox chemistry of rapid and reversible transformation between its oxide and metallic states.

We are now reporting a work-in-progress combining a series of adsorption and catalytic reactions for converting adsorbed CO_2 emitted from power plant oxygen-containing flue gas where the redox property of Ru/RuO_x is critical for successful use. The material used for this process is composed of a nano-dispersed [24] alkaline component in intimate contact with Ru on a high surface area carrier (Al_2O_3), referred to as a Dual Function Material (DFM). It adsorbs CO_2 on its alkaline component and catalytically converts it to synthetic natural gas (i.e., CH_4) in the subsequent step over the Ru catalyst approaching a closed loop for carbon utilization. The sequential steps will be discussed below.

Alkaline carbonates have been reported to be efficient for CO_2 adsorbents [25]. What is the most relevant to our new materials is the ability to adsorb CO_2 and then hydrogenate catalytically to methane. The catalytic hydrogenation of a series of carbonates was first reported by Tsuneto et al. in 1992 [26] and Yoshida et al. in 1999 [27]. A variety of transition metal catalysts (but not Ru) were physically mixed with the carbonates and hydrogenation was conducted. The carbonate was completely hydrogenated but there was no attempt to reform the carbonate by CO_2 capture.

We have demonstrated that a DFM, containing 5% Ru, 10% Na_2CO_3/Al_2O_3, captures CO_2 both on the carbonate surface and depleted bulk carbonate sites, which are subsequently hydrogenated to CH_4. In a typical implementation of this material, the methane produced is dried and compressed and recycled to the inlet of the power plant or integrated into the natural gas grid, ideally closing the carbon cycle. Thus, this material provides an additional source of sites for CO_2 capture by carbonate reformation, yielding an increase in subsequent methane production. For this scheme to be used, H_2 used for methanation needs to be generated from water electrolysis, the energy of which is provided by excess solar or wind energy [22]. Installations for water electrolysis powered by solar energy for H_2 vehicle fueling stations has been announced between Guangdong Synergy Hydrogen Power Technology (Guangdong, China) and Proton On Site (Wallingford, CT, USA). Installations in Foshan and Yunfu, cities in China, will be initial locations [28]. Thus it is expected that renewable H_2 will be available in selected locations.

The two-step sequential reactions involve first the selective adsorption of CO_2 from O_2-containing flue gas on the DFM. During this step, the Ru in the DFM is oxidized to RuO_x. Upon CO_2 saturation, the flue gas is diverted to an identical parallel reactor where CO_2 capture continues. Renewable H_2 is added to the reactor containing the saturated DFM where it rapidly reduces the RuO_x to its metallic and active state, and methanation proceeds via CO_2 spill over to the Ru sites. All steps are conducted at the same temperature (~320 °C) [29]. Therefore, the reversibility of the redox chemistry of Ru/RuO_x

makes it unique for this process relative to commonly used Ni, which when oxidized will not reduce under the conditions of this process [30–32].

This paper reports cyclic aging studies from a simulated flue gas demonstrating stable repeatable cycles of CO_2 adsorption and methanation. The importance of H_2 exposure intensity will also be discussed. The price of Ru should not be confused the more expensive among precious metal catalysts. Its price per gram as of 21 December 2016, was Ru $1.25, Rh $24.53, Pt $28.40, and Pd $20.60 with all recycled for continued use.

2. Results and Discussion

2.1. Na_2CO_3 Loading Study

Various carbonate-containing materials were evaluated on a thermal gravimetric analysis (TGA) for reversible CO_2 adsorption. The CO_2 adsorbed and methanation in mmol per gram on Al_2O_3 supported K_2CO_3, Na_2CO_3, and MgO powder adsorbents with weight loadings from 5% to 20% were previously reported [30]. In this study K_2CO_3 and Na_2CO_3 showed the largest CO_2 adsorption relative to Al_2O_3 supported CaO and MgO. 10% Na_2CO_3 on Al_2O_3 achieved the highest adsorption capacity (0.11 mmol/g), and was therefore selected for additional adsorption studies. Figure 1 shows TGA results for CO_2 adsorption and reversible desorption for dispersed Na_2CO_3 on Al_2O_3 at different loadings.

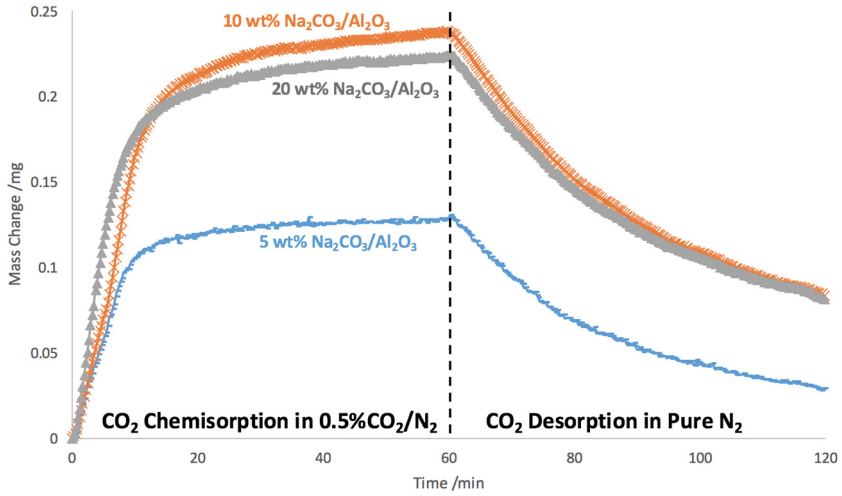

Figure 1. Thermal Gravimetric Analysis (TGA) adsorption studies conducted at 320 °C for 50 mg of powder. Before the adsorption the samples were degassed in 2% H_2/N_2 for 2 h, then exposed to 0.5% CO_2 in N_2 and subsequently pure N_2.

Figure 1 indicates 10 wt % Na_2CO_3/Al_2O_3 obtained the highest capacity of CO_2 adsorption (0.11 mmol/g) among other Na_2CO_3 loadings. The pure N_2 purge verifies that Na_2CO_3 dispersed on γ-Al_2O_3 powder has the ability of desorb the CO_2 reversibly in situ, consistent with dispersed CaO/Al_2O_3 substantiating that the binding interaction between CO_2 and adsorbents is weak [33]. This property insures the desorption and spill-over of CO_2 to Ru catalytic sites for methanation.

Based on the methanation capacities, DFM composed of 5% Ru, 10% Na_2CO_3/Al_2O_3 generated the most methane (1.05 mol CH_4/kg of DFM) compared to other adsorbents at the same loading [30]. Herein, further studies were conducted on Al_2O_3 supported Ru-Na_2CO_3 DFM.

2.2. Carbonate Hydrogenation Study

A H_2 activation (reduction) step was conducted using unsupported Ru-Na_2CO_3 to understand the decomposition profile of Ru nitrosyl nitrate used in the powder preparation procedure. However,

a greater weight loss than expected was observed indicating hydrogenation of the carbonate in the sample was also occurring. Results all conducted at 320 °C using the TGA is shown in Figure 2 in which the final step shows CO_2 adsorption.

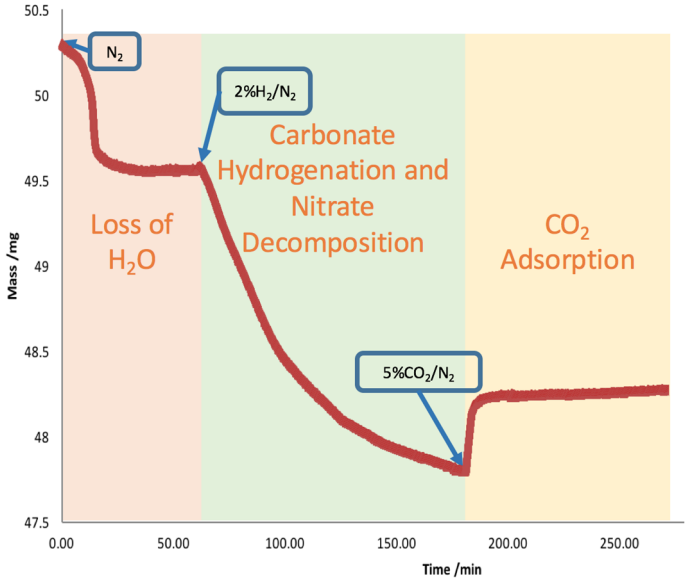

Figure 2. TGA result of Ru salts and carbonate hydrogenation study operated at 320 °C for 50 mg of 1.44% Ru/Na_2CO_3 powder sample.

During the sample preparation, the 50 mg of 1.44% Ru/Na_2CO_3 was dried at 120 °C for 2 h and calcined at 250 °C for 2 h in air. When the precursor Ru(NO)$(NO_3)_3$ is heated, it has been reported that a mixture of oxides such as RuO, RuO_2, RuO_3, and RuO_4 [33,34] form depending on the temperature.

After a one-hour N_2 purge at 320 °C, the sample achieved stable weight as water and/or other volatile components evaporated. At this point, 2% H_2/N_2 was introduced. During the two-hour H_2 exposure, Ru is expected to reduce, nitrate decompose, and some carbonate hydrogenate. The stable weight decreased by 1.763 mg. Assuming the Ru(NO)$(NO_3)_3$ remained in its original form as it is in the precursor, the expected weight loss would be 1.332 mg or 65.37% of the total mass loss. Therefore, the residual mass loss (an additional 34.63%) can be explained by carbonate hydrogenation catalyzed by the newly formed Ru metal. It is clear from Figure 2 that a continuing weight loss likely occurs due to the slow hydrogenation of the carbonate. After about 120 min of pretreatment, the sample showed an ability to re-adsorb CO_2 in depleted sites, replacing some of that which was hydrogenated.

2.3. Hydrogen Exposure Time Study

50 mg of 5% Ru, 10% Na_2CO_3/Al_2O_3 powder sample was subjected to a one-hour pretreatment in 2% H_2/N_2 at 320 °C. In Figure 3, a rapid adsorption of CO_2 up to 1.2 mg from a feed gas of 5% CO_2 in N_2 was observed. Upon the addition of 2% H_2/N_2 three distinct slopes of weight loss vs time are observed. The largest slope, between 30 and 35 min, was 0.086 mg/min. The second between roughly 35 and 70 min was 0.00952 mg/min and the third about 0.00195 mg/min from 70 to 660 min. The first loss, associated with the largest slope, occurs from 1.2 mg to 0.66 mg is likely due to methanation of the CO_2 adsorbed on the Ru metal. This weight loss is approximately 50% of the Ru atoms present assuming 1 CO_2 adsorbed per Ru site. It is also possible 1 CO_2 adsorbs on two Ru sites for dissociative adsorption to CO and atomic O [23]. The second slope has a weight loss of about 0.45 mg which is twice that observed for CO_2 adsorbed on 10% Na_2CO_3/Al_2O_3 (see Figure 1) suggesting that additional sites for CO_2 adsorption have become available due to the depleted sites generated by the hydrogenation of the bulk carbonate itself upon the addition of H_2. The second slope is speculated to be the hydrogenation weakly adsorbed CO_2 on the carbonate surface most of which

has spilled over to the Ru sites where the heat liberated (not shown) is indicative of methanation. The weight loss associated with the lowest slope is less than 0.2 mg as is believed to be hydrogenation of the bulk carbonate. This is speculative, since Figure 1 was generated with a feed gas of only 0.5% CO_2/N_2 while Figure 3 was conducted with 5% CO_2/N_2. However, CO_2 chemisorption reaches a plateau where it becomes independent of partial pressure.

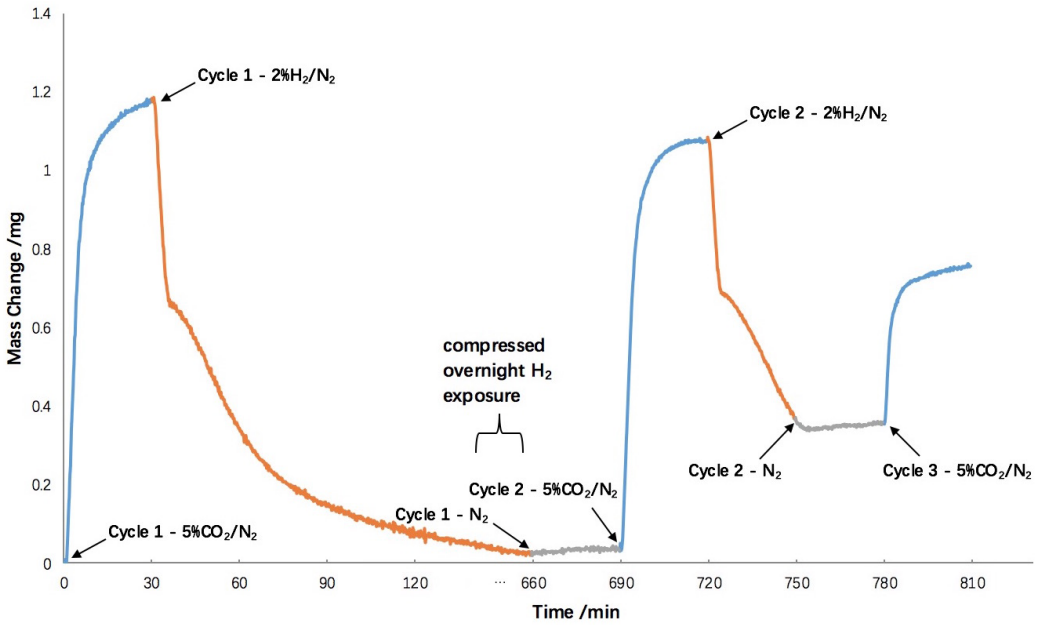

Figure 3. TGA result of the 3-cycle test for 50 mg of 5% Ru, 10% Na_2CO_3/Al_2O_3 at 320 °C. The plot excluded the over-night activation step at 320 °C in 2% H_2/N_2. The long tail of low weight loss in the first cycle was compressed indicating an overnight (10.5 h) hydrogen exposure at 320 °C.

For the 2nd cycle, the mass gain for CO_2 adsorption was similar to the first cycle. However, with only 30 min of hydrogen exposure, the weight loss was significantly less than after the longer time exposure in cycle 1. In the third cycle it is likely only the Ru metal and the surface of Na_2CO_3 adsorb CO_2 since insufficient hydrogenation of the bulk carbonate had occurred with only a 30-min exposure. It is clear that bulk carbonate hydrogenation is dependent on exposure time and hydrogen partial pressure. This will be demonstrated in the following studies.

2.4. 10-Cycle Test in CO_2 Feed

Although the primary commercial target of our research is focused on power plant exhaust gases containing O_2 and steam, there are applications where they are not present, such as fermentation, land fill, and cement manufacturing effluents. Therefore, an aging test consisting of 10 cycles using 7.5% CO_2/N_2 for the adsorption was conducted in our scaled up reactor with DFM pellets. This is more consistent with industrial processes since fine powdered materials create operational, technical and health problems for workers. For example, in a fixed bed reactor, powders have high pressure drop [35] and expose operators to possible risk of chronic human health issues such as respiratory problems and lung cancer [36]. In order to avoid such issues and facilitate commercialization, a process was conducted with 10 grams of freshly prepared pelleted DFM (5 mm × 5 mm tablets of γ-Al_2O_3) and cycle tested in a larger scale fixed bed reactor.

The results for CO_2 adsorption and methanation under O_2-free conditions are shown in Figure 4. Given the slow kinetics for bulk carbonate hydrogenation experienced in Figure 3, the H_2 was increased to 5% H_2/N_2. The Ru-Na_2CO_3 DFM achieved stable adsorption and methanation performance for 10 successive cycles and is expected to maintain this advantage over many more cycles. However,

the average conversion efficiency of the adsorbed CO_2 converted to methane was only 60.5%. A large amount of desorbed CO_2 was observed at the reactor outlet. The 39.5% unreacted CO_2 released is likely due to its premature desorption caused by the large exotherm of methanation. We intend to address this by performing parametric studies for feed gas components (i.e., H_2 partial pressure) and process variations. It is also logical to locate a small Ru catalyst downstream to complete methanation of the unconverted CO_2. Conditions of our experiments were controlled to avoid CO formation. CO is only produced at higher temperatures and space velocities over Ru as shown in reference [23].

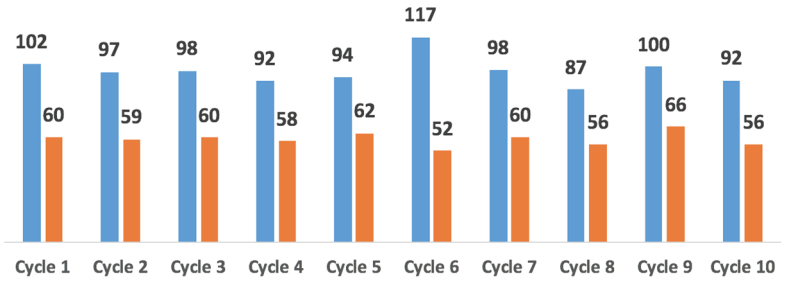

Figure 4. CO_2 adsorption and methanation cycles (10) using 10 grams of the Ru-Na_2CO_3 DFM (5% Ru, 10% Na_2CO_3/Al_2O_3) pellets in a fixed packed bed reactor with 7.5% CO_2/N_2 at 320 °C. A 150-min of 5% H_2/N_2 exposure was used during pretreatment followed by 10 identical CO_2 adsorption-methanation cycles. 5% H_2/N_2 for 30 min was used for the methanation cycles. The volumes of CO_2 adsorbed and CH_4 produced are shown in the figure.

2.5. 12-Cycle Test in Simulated Flue Gas

Performance of the pelleted Ru-Na_2CO_3 DFM in simulated O_2-and-steam-containing flue gas is another key factor for its commercialization and application. A 12-cycle test was conducted in the fixed bed reactor with the performance shown in Figure 5. The results of BET specific surface area of the fresh and after-12-cycle Ru-Na_2CO_3 pelleted DFM sample is shown in Table 1, in which the small change is consistent with the stable performance of the sample. Table 1 reports the BET and Ru crystallite sizes for fresh and cyclic aged DFM. Some sintering is observed. However, given the low temperatures of the process, this is not expected to be a major source of deactivation. Extended cyclic aging will be necessary to more definitively determine the major sources of deactivation. These studies will be soon initiated. Crystallite sizes (d) were calculated from the equation $d = (103/\%D)$ where $\%D$ = % dispersion and 103 is the constant related to the number of Ru atoms present in the samples determined from room temperature H_2 chemisorption [37].

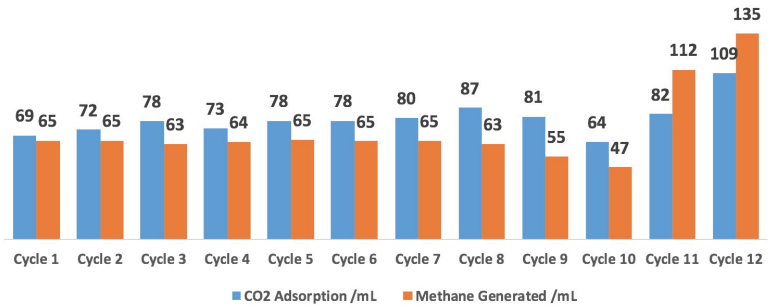

Figure 5. CO_2 adsorption and methanation using 10 grams of the Ru-Na_2CO_3 DFM (5% Ru, 10% Na_2CO_3/Al_2O_3) pellet for the 12-cycle test conducted in the fixed bed reactor in simulated flue gas at 320 °C. Pretreatment of the DFM was conducted with 5% H_2/N_2 for 150 min before the first cycle. For cycles 2–10, hydrogen exposure was 30 min. Before cycle 11 another 150-min 5% H_2/N_2 exposure was added, and for cycle 12, 48 h H_2 exposure. The volumes shown in the figure are for CO_2 adsorbed and CH_4 produced.

Table 1. Brunauer-Emmett-Teller (BET) specific surface area of the fresh and flue gas cyclic aged Ru-Na_2CO_3 DFM pellets. Ru crystallite sized for fresh and cyclic aged samples based on H_2 chemisorption assuming H/Ru = 1/1.

Sample	BET Specific Surface Area (m^2/g)	Ru Crystallite Sizes (nm)
Fresh Ru-Na_2CO_3 DFM pellet	103	3.98
Flue gas cyclic aged Ru-Na_2CO_3 DFM pellet	89	5.15

The CO_2 adsorption capacity was reduced compared to the O_2 free process of Figure 4, because Ru was inactivated—for CO_2 adsorption—to RuO_x by O_2 in the simulated flue gas. Both adsorption and methanation capacity remained relatively stable until the 9th cycle, when reduction in both CO_2 adsorption and CH_4 produced was noted. Since both CO_2 adsorption and methanation are linked to Ru activity, it was reasonable to assume that the RuO_x was not sufficiently reduced, causing a loss in both performances.

Before the 11th cycle, the material was given an extra 150-min of hydrogen exposure, resulting in a recovery of both CO_2 adsorption and methanation. When the extra hydrogen exposure was extended to 48 h before the 12th cycle, both capacities reached even higher levels. This apparent deactivation was not observed in the O_2 free cycle tests of Figure 4. This again demonstrated the importance of H_2 partial pressure in maintaining Ru reduced while enhancing the rate of bulk carbonate hydrogenation.

The average conversion of adsorbed CO_2 converted to methane during the 12-cycle test was 89.6%, which is a great improvement compare to the 10-cycle test in the dry CO_2 feed (60.5%). Though the overall CO_2 adsorption of the 12-cycle test in the simulated flue gas was lower than in the 10-cycle test, the conversion efficiency of 12-cycle test is preferred. Water generated at the surface during methanation may oxidize the surface of Ru. Therefore, a minimum H_2 partial pressure is required to maintained Ru in the reduced and active state. We have found that H_2 partial pressure is a critical parameter necessary for reducing the RuO_x formed during CO_2 adsorption (Figure 5) and methanation (Figure 6). This will be confirmed in the future.

2.6. Effect of H_2 Partial Pressure on CO_2 Hydrogenation and RuO_x Reduction

As observed for Figure 5, the loss in performance was reversed by increasing the exposure time of the DFM to H_2. It is reasonable to assume that increasing the partial pressure of H_2 would have the same effect by maintaining the Ru in the metallic and active state while increasing the extent of carbonate hydrogenation. This was demonstrated in Figure 6 where 10% H_2/N_2 dramatically increased the amount of methane produced (131 mL) compared to 5% H_2/N_2 (58.7 mL). This also points to the importance of the redox chemistry of Ru/RuO_x. It is logical to assume that during the 12-cycle simulated flue gas test (Figure 5), Ru was oxidized and there was insufficient H_2 to re-reduce it.

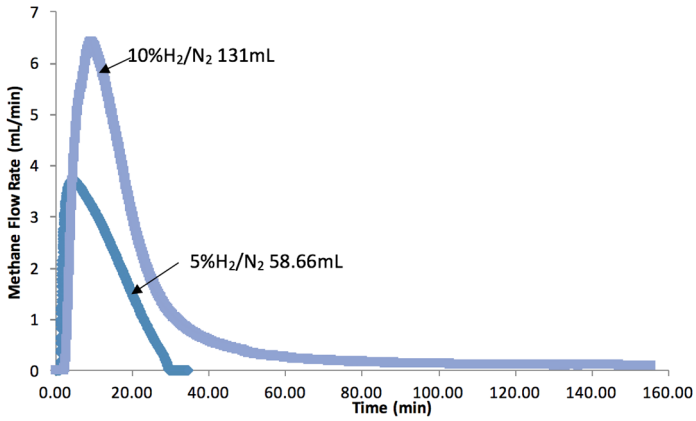

Figure 6. Methane production comparison of 5% H_2/N_2 and 10% H_2/N_2. The test was operated using 10 grams of 5% Ru, 10% Na_2CO_3/Al_2O_3 pellets in the large fixed bed reactor. The operational conditions were at 320 °C, 300 mL/min of 7.5% CO_2/N_2 for CO_2 adsorption. The volume of methane produced are shown.

The rate and extent of RuO_x reduction is critical for the flue gas operation. In TGA experiments the rate and extent of RuO_x reduction was to understand the minimum H_2 content needed for rapid reduction of the oxides of Ru. Results are shown in Figure 7. It is clear the reduction rate (slope) increases with H_2 content (0.069 mg/min at 1.30% H_2 to 0.370 mg/min at 2.86% H_2). The most dramatic increase occurs for H_2 > 1.3%. Equally as significant is the decrease in time for initiation of reduction as the H_2 content increases. This points to the reducibility of RuO_x to Ru, making it more suitable for the DFM flue gas process relative to NiO_x to Ni metal [32] that requires temperatures in excess of 500 °C for reduction.

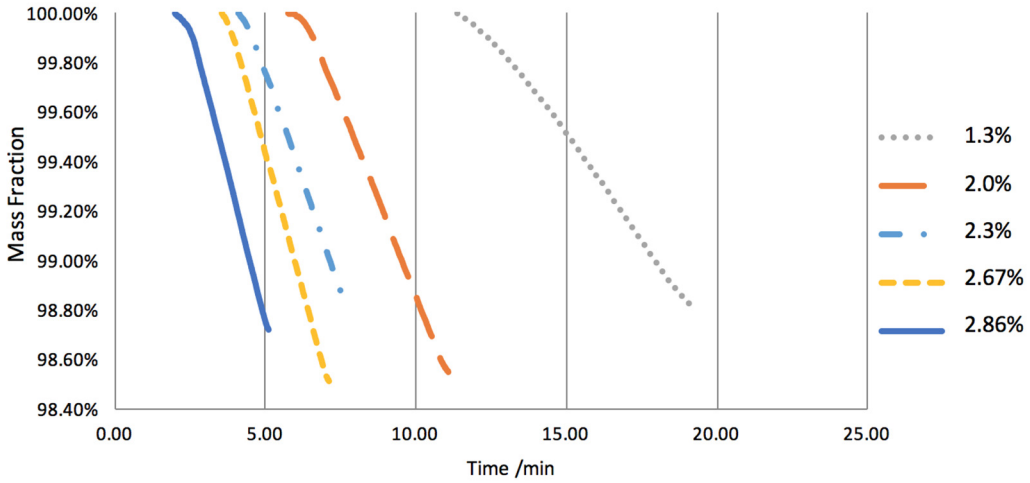

Figure 7. TGA results of RuO_x reduction on 50 mg 5% Ru/Al_2O_3 powder samples H_2 partial pressures from 1.3% to 2.86% at 300 °C. Only reduction sections are shown in the figure.

2.7. Speculated Functional Pathway of the Ru-Na_2CO_3 DFM

The speculated pathways for each step and component in DFM are summarized in Table 2. The RuO_x, as prepared, must be activated to its active metallic state for methanation. For feeds containing O_2, it will be oxidized and lose its ability to adsorb CO_2. However, during methanation it will be reduced and re-activated for methane production. For O_2-free feed gas, Ru is both active for CO_2 adsorption and methanation.

Table 2. Speculated function pathway of Ru and Na_2CO_3 in the Ru-Na_2CO_3 DFM.

Section	Ru Pathway	Na_2CO_3 Pathway
Pretreatment	$RuO_x + xH_2 \rightarrow Ru + xH_2O$	$Na_2CO_3 + 4\,H_2 \overset{Ru}{\rightarrow} 2\,NaOH + CH_4 + H_2O$
O_2-free CO_2 feed [1]	$Ru + CO_2 \rightarrow Ru\cdots CO_2$	$4\,NaOH + 4\,CO_2 \rightarrow Na_2CO_{3\ bulk} + Na_2CO_{3\ surface}\cdots CO_2 + 2\,H_2O$
O_2-containing CO_2 feed	$Ru + \frac{x}{2}O_2 \rightarrow RuO_x$	$4\,NaOH + 4\,CO_2 \rightarrow Na_2CO_{3\ bulk} + Na_2CO_{3\ surface}\cdots CO_2 + 2\,H_2O$
Methanation & hydrogenation	$RuO_x + xH_2 \rightarrow Ru + xH_2O$	$Na_2CO_{3\ surface}\cdots CO_2 + 8\,H_2 \overset{Ru}{\rightarrow} 2\,CH_4 + H_2O + Na_2CO_{3\ surface}$ $Na_2CO_{3\ bulk} + 4\,H_2 \overset{Ru}{\rightarrow} 2\,NaOH + CH_4 + H_2O$

[1] $Na_2CO_{3\ bulk}$ and $Na_2CO_{3\ surface}$ are the same component but bulk and surface are distinguished.

For Ru-Na_2CO_3 DFM, bulk carbonate hydrogenation occurs during pretreatment, producing NaOH and CH_4 with CO_2 spill-over to Ru sites. Upon exposure to CO_2, it is reformed to a bulk carbonate species where CO_2 adsorbs on the surface $Na_2CO_3\cdots CO_2$ and reforms bulk carbonate. The slowest step is the hydrogenation of the reformed bulk carbonate. Table 2 is still speculative and is the focus of on-going kinetic and characterization studies.

3. Experimental

3.1. Material Synthesis

The powder materials tested were prepared via incipient wetness method on a high surface area γ-Al_2O_3 (SBA-150, BASF, Iselin, NJ, USA) support using ruthenium(III) nitrosylnitrate ($Ru(NO)(NO_3)_3$, Ru 31.3% min, Alfa Aesar, Tewksbury, MA, USA) and Na_2CO_3 (Sigma-Aldrich, St. Louis, MO, USA) as the precursors for Ru and Na_2CO_3, respectively. Repeated impregnations were conducted to reach the designed loadings if necessary. The Al_2O_3 supported alkaline materials (Na_2CO_3) were dried at 120 °C for 2 h and then calcined at 400 °C for 4 h in air. For Ru deposition, the material was dried at 120 °C for 2 h followed by calcination at 250 °C for 2 h in air after metal catalyst (Ru) impregnations.

The pellet materials (5 mm × 5 mm tablets) used for the cyclic tests were prepared via a precipitation method with the target composition of 5% Ru, 10% Na_2CO_3/Al_2O_3 (TH100, SASOL, Hamburg, Germany). The principle procedure of the precipitation method was derived from the work done by Zheng et al. [31], but the impregnation order, selected precursors, and calcination programs were modified (see Figure 8 for the preparation process flow). Ruthenium(III) chloride hydrate ($RuCl_3 \cdot xH_2O$, 99.9% PGM basis, Ru 38% min, Alfa Aesar, Tewksbury, MA, USA) and sodium carbonate (Sigma-Aldrich) were the chosen precursors for Ru and Na_2CO_3, respectively. Using $RuCl_3$ as the Ru precursor for pellet sample instead of $Ru(NO)(NO_3)_3$ achieved more uniform penetration within the pellets, consequently improved dispersion of Ru, and avoided residual of precursor in the sample. The highest calcination temperature was 250 °C to avoid generation of high temperature volatile ruthenium oxides (>300 °C in air). The water wash was introduced, after precipitation of water-insoluble $Ru(OH)_x$ to remove unwanted chlorides. The carbonate salts were then impregnated and processed as shown in Figure 8.

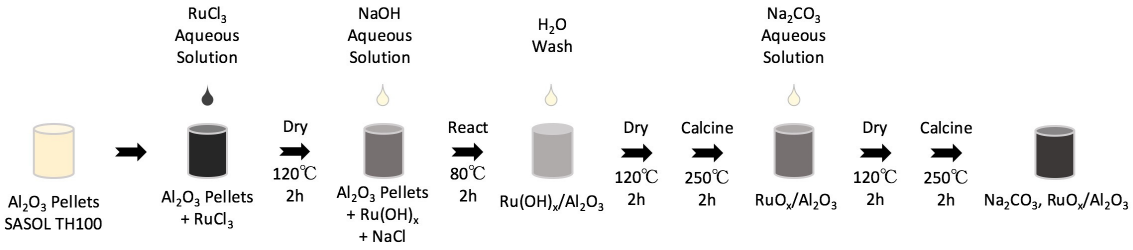

Figure 8. Ru-Na_2CO_3 DFM pellet preparation process flow using the precipitation method. A slight excess of NaOH was used with a ratio of Ru:OH = 1:4.5 to precipitate $Ru(OH)_x$. A water wash and filtration (40 times of water immersion and separation) was used to remove any NaCl. Drying and calcination steps were conducted in air.

3.2. Thermogravimetric Analysis (TGA)

Thermogravimetric analysis were conducted using either a TG 209 F1 Libra NETZSCH or SAT 449 F3 Jupiter NETZSCH unit for the Na_2CO_3 loading, carbonate hydrogenation, and hydrogen exposure time study. For each test, 50 mg of the prepared powder sample was placed in an alumina crucible and located in the instrument. The temperatures for carbonate hydrogenation and nitrate decomposition, CO_2 adsorption/desorption, and CO_2 methanation, were all conducted at 320 °C, while the feed gases and corresponding time periods were varied. Table 3 shows the programs in detail for each test. The total flow rates were always 40 mL/min for each feed gas. Before each test, the sample was heated to 320 °C in pure nitrogen until a stable final weight was observed. Hydrogen was introduced in pre-treatments to decompose the ruthenium nitrate to active metallic ruthenium while decomposing the remaining nitrate compounds until stable mass was observed. Pure nitrogen was used only to de gas each sample.

Table 3. Programs of TGA tests at 320 °C related to the results discussed in this paper.

Test	Pre-Treatment	Step 1	Step 2	Step 3
Na_2CO_3 Loading Study	2% H_2/N_2, 2 h	0.5% CO_2/N_2, 1 h	Pure N_2, 1 h	-
Carbonate Hydrogenation Study	Pure N_2, 1 h	2% H_2/N_2, 2 h	5% CO_2, 2 h	-
Hydrogen Exposure Time Study [1]	2% H_2/N_2, 1 h	5% CO_2/N_2, 30 m	2% H_2/N_2, 10.5 h	Pure N_2, 30 m

[1] The step 2 shows in the table was for the first cycle of the test only. For the 2nd and the 3rd cycle, step 2 lasted only for 30 min, while the other steps were the same as it was in cycle 1.

3.3. Scaled-Up Fixed Bed Reactor

Cyclic tests of CO_2 adsorption and catalytic conversion to methane in a fixed bed reactor are shown in Figure 9. The reactor consisted of gas feed system, furnace, fixed bed reactor, and product analyzer. The gas feed system includes cylinders of compressed designed gases (TechAir, White Plains, NY, USA), rotameters (Key Instruments, Hatfield, PA, USA) calibrated with a precise bubble meter for flow rate control, and a syringe pump (Cole-Parmer, Vernon Hills, IL, USA) along with heating tape (maintains temperature at 125 °C) for steam introduction. The fixed bed reactor is housed in a microthermal furnace (MTSC12.5R-0.75x18-1Z-IOT, Mellen, Concord, NH, USA) and is composed of a standard quartz tube (O.D. = 25 mm, I.D. = 20 mm, length = 570 mm), a thermocouple (*K*-type, Omega, Norwalk, CT, USA) was placed at gas inlet. An uncoated ceramic monolith was used to secure the pellets and glass beads (DI of 6 mm, Fisher Scientific, Hampton, NH, USA), the latter used to fill the downstream dead volume. Water (steam) in the gas outlet, from the feed gas and water produced from methanation, was condensed by an ice cold trap before flowing into the analytical unit. The exhaust gas analyzer was an Enerac Model 700 equipped with electrochemical sensors for CO, CO_2, and hydrocarbons, and nondispersive-infrared sensor for O_2. It operates with a frequency of 1 Hz, allowing gas measurements every one second. No pressure drop was observed during the reactor tests from the inlet to the outlet.

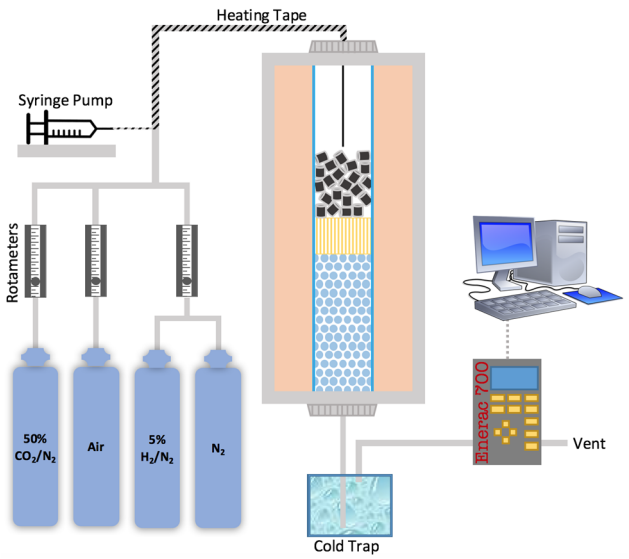

Figure 9. Diagram of scaled-up fixed bed reactor. The N_2 cylinder was used either exclusively or simultaneously with the 50% CO_2/N_2 cylinder to dilute the CO_2 concentration to 7.5% for feeding. The computer connected to the Enerac unit equipped with infrared/electrochemical sensors recorded data every second. Total flow rate of each gas feeding was 300 mL/min.

The two cyclic tests each contained 10 grams of 5% Ru, 10% Na_2CO_3/Al_2O_3 pellets at 320 °C and 300 mL/min (GHSV = 1432 h^{-1}) for total flow rates. The process flow for each cycle in these two tests is shown in Figure 10. The pre-reduction step for both was designed to reduce the RuO_x to Ru metal during preparation. For the 10-cycle test, only 7.5% CO_2 in N_2 was used for the CO_2 adsorption step.

No N_2 purge between adsorption and methanation was needed since no O_2 was present in this series of tests.

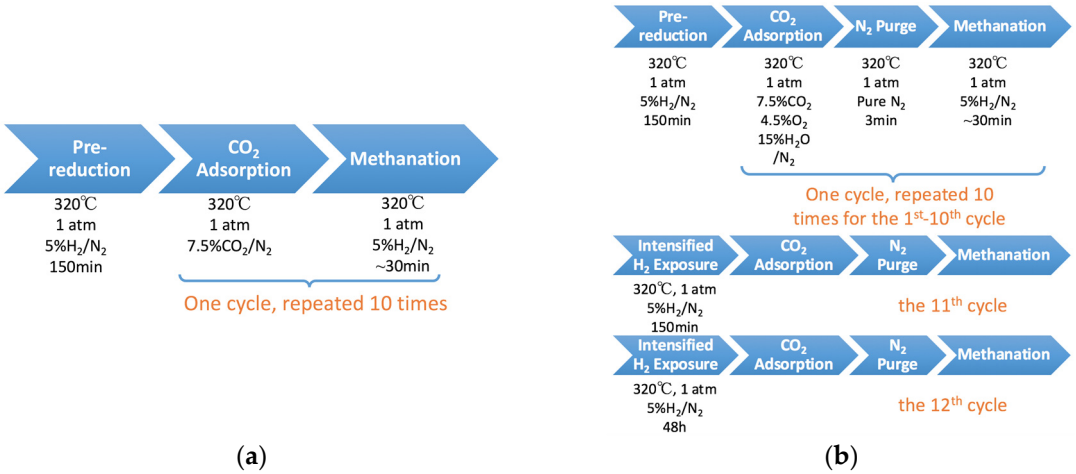

Figure 10. Process flow for the two different cyclic tests operated on the scaled-up fixed bed reactor. (**a**) O_2- and steam-free CO_2 adsorption and hydrogenation for the 10-cycle test. Pre-reduction was utilized only once before the first cycle. The subsequent ten cycles were conducted repeatedly under identical experimental conditions; (**b**) Simulated flue gas 12-cycle test with the pretreatment used only before the first cycle followed by 10 identical cycles. A N_2 purge was needed between each cycle to avoid H_2-O_2 contact. Before the 11th and the 12th cycle, a prolonged H_2 exposure was utilized while subsequent steps remained the same as the first ten cycles.

The 12-cycle test was performed in simulated natural gas fired power plant flue gas, containing 7.5% CO_2, 4.5% O_2, 15% H_2O and balance N_2. A 3-min N_2 purge between CO_2 adsorption and methanation and the reverse was added to avoid contact of H_2 and O_2. The first ten cycles were operated continuously and identically, while the last two cycles required a prolonged H_2 purge before CO_2 feed was introduced. The 11th cycle underwent a 150 min 5% H_2/N_2 exposure and the 12th for 48 h. The prolonged H_2 exposure was needed to regenerate the re-oxidized ruthenium.

4. Conclusions

The bulk carbonate present in Ru-Na_2CO_3 DFM can adsorb and convert CO_2 to CH_4. Additionally, the bulk carbonate can also be catalytically hydrogenated to CH_4 providing "depleted" sites for additional CO_2 adsorption from flue gases. Ru plays a key role as a methanation catalyst for O_2-containing flue gas due to its ease of reduction once oxidized. Once in its reduced state it provides an additional site for CO_2 capture as well as effective methanation. This technology overcomes some of the limitations of aqueous amine CO_2 scrubbing by having the dual capability of both capturing CO_2 in O_2-flue gas and subsequently methanating the CO_2 at one temperature using renewable H_2. The methane produced is dried, compressed, and recycled to the front of the plant ideally closing the carbon balance, with conversion of 89.6% of the captured CO_2 in simulated flue gas.

The Ru-Na_2CO_3 DFM demonstrated stable performance for at least 10 cycles of CO_2 adsorption and methanation in an O_2-free CO_2 feed gas. In simulated flue gas, due to the presence of oxygen, part of active metallic Ru is oxidized and loses its activity for CO_2 adsorption and methanation. Stable performance was observed in the flue gas up to the point where Ru becomes less effective due to oxidation. This apparent deactivation can be reversed by prolonged exposure to H_2 or preferably by a high H_2 content. The reversibility is due to the ease of reduction of RuO_x to Ru.

Acknowledgments: Financial support from AngloAmerican is greatly appreciated. The authors would like to thank SASOL and BASF for their material support.

Author Contributions: The present work was conducted under the supervision of Robert J. Farrauto, with Shuoxun Wang, Erik T. Schrunk, and Harshit Mahajan as authors at Columbia University. Robert J. Farrauto did the main research consulting and paper editing, and is named the correspondent author of the submitted work. Shuoxun Wang (Ph.D. candidate) designed and conduct most of the experiments and paper writing, and is named the primary author. Erik T. Schrunk helped with the experimental designs and operations on the scaled-up fixed bed reactor. Harshit Mahajan completed the experiment of RuO_x reduction.

Conflicts of Interest: The authors declare no conflict of interest.

References

1. Stewart, C.; Hessami, M.-A. A study of methods of carbon dioxide capture and sequestration—-The sustainability of a photosynthetic bioreactor approach. *Energy Conver. Manag.* **2005**, *46*, 403–420. [CrossRef]
2. Hasib-ur-Rahman, M.; Siaj, M.; Larachi, F. Chemical Engineering and Processing: Process Intensification. *Chem. Eng. Process. Process Intensif.* **2010**, *49*, 313–322. [CrossRef]
3. Audus, H.; Freund, P.; Smith, A. *Global Warming Damage and the Benefits of Mitigation*; IEA Greenhouse Gas R&D Programme: Paris, France, December 1995.
4. Heintz, Y.J.; Sehabiague, L.; Morsi, B.I.; Jones, K.L.; Pennline, H.W. Novel Physical Solvents for Selective CO_2 Capture from Fuel Gas Streams at Elevated Pressures and Temperatures. *Energy Fuels* **2008**, *22*, 3824–3837. [CrossRef]
5. Carmo, M.; Fritz, D.L.; Mergel, J.; Stolten, D. A comprehensive review on PEM water electrolysis. *Int. J. Hydrog. Energy* **2013**, *38*, 4901–4934. [CrossRef]
6. Ursua, A.; Gandia, L.M.; Sanchis, P. Hydrogen Production from Water Electrolysis: Current Status and Future Trends. *IEEE Proc.* **2012**, *100*, 410–426. [CrossRef]
7. Lackner, K.S. A guide to CO_2 Sequestration. *Science* **2003**, *300*, 1677–1678. [CrossRef] [PubMed]
8. Saeidi, S.; Amin, N.A.S.; Rahimpour, M.R. Hydrogenation of CO_2 to value-added products—A review and potential future developments. *J. CO_2 Util.* **2014**, *5*, 66–81. [CrossRef]
9. Spigarelli, B.P.; Kawatra, S.K. Opportunities and challenges in carbon dioxide capture. *J. CO_2 Util.* **2013**, *1*, 69–87. [CrossRef]
10. Rochelle, G.T. Amine Scrubbing for CO_2 Capture. *Science* **2009**, *325*, 1652–1654. [CrossRef] [PubMed]
11. Buelens, L.C.; Buelens, L.C.; Galvita, V.V.; Poelman, H.; Detavernier, C.; Marin, G.B. Super-dry reforming of methane intensifies CO_2 utilization via Le Chatelier's principle. *Science* **2016**, *354*, 449–452. [CrossRef] [PubMed]
12. Bobadilla, L.F.; Riesco-García, J.M.; Penelás-Pérez, G.; Urakawa, A. Enabling continuous capture and catalytic conversion of flue gas CO_2 to syngas in one process. *J. CO_2 Util.* **2016**, *14*, 106–111. [CrossRef]
13. Bartholomew, C.; Farrauto, R.J. *Fundamentals of Industrial Catalytic Processes*; Wiley and Sons: New York, NY, USA, 2006; Chapter 7; pp. 490–491.
14. Bartholomew, C.; Farrauto, R.J. *Fundamentals of Industrial Catalytic Processes*; Wiley and Sons: New York, NY, USA, 2006; Chapter 6; p. 355.
15. Bilgrien, C.; Davis, S.; Drago, R. The selective oxidation of primary alcohols to aldehydes by oxygen employing a trinuclear ruthenium carboxylate catalyst. *J. Am. Chem. Soc.* **1987**, *1987*, 3786–3787. [CrossRef]
16. Huang, Y.Y.; Yang, X.; Feng, Y.; Verpoort, F.; Fan, Q.H. Chiral Ru/Ir bimetallic dendronized polymer catalysts constructed through sequential metal coordination and applied in asymmetric hydrogenation of quinaldine. *J. Mol. Catal. A Chem.* **2014**, *393*, 150–155. [CrossRef]
17. Saadatjou, N.; Jafari, A.; Sahebdelfar, S. Ruthenium Nanocatalysts for Ammonia Synthesis: A Review. *Chem. Eng. Commun.* **2014**, *202*, 420–448. [CrossRef]
18. Shen, L.; Zhang, C.; Liu, Y. Meso-macroporous Al_2O_3 supported Ru catalysts for CO preferential oxidation in hydrogen-rich gases. *J. Nat. Gas Chem.* **2012**, *21*, 653–660. [CrossRef]
19. Steynberg, A.P.; Dry, M.E. *Fischer-Tropsch Technology, Studies in Surface Science and Catalysis*; Elsevier: Amsterdam, The Netherlands, 2004; Chapter 7; pp. 560 and 566.
20. Menzel, N.; Ortel, E.; Mette, K.; Kraehnert, R.; Strasser, P. Dimensionally stable Ru/Ir/TiO_2-anodes with tailored mesoporosity for efficient electrochemical chlorine evolution. *ACS Catal.* **2013**, *3*, 1324–1333. [CrossRef]

21. Garbarino, G.; Bellotti, D.; Riani, P.; Magistri, L.; Busca, G. Methanation of carbon dioxide on Ru/Al_2O_3 and Ni/Al_2O_3 catalysts at atmospheric pressure: Catalysts activation, behaviour and stability. *Int. J. Hydrog. Energy* **2015**, *40*, 9171–9182. [CrossRef]
22. Götz, M.; Lefebvre, J.; Mörs, F.; McDaniel Koch, A.; Graf, F.; Bajohr, S.; Reimert, R.; Kolb, T. Renewable Power-to-Gas: A technological and economic review. *Renew. Energy* **2016**, *85*, 1371–1390. [CrossRef]
23. Janke, C.; Duyar, M.S.; Hoskins, M.; Farrauto, R. Catalytic and adsorption studies for the hydrogenation of CO_2 to methane. *Appl. Catal. B Environ.* **2014**, *152–153*, 184–191. [CrossRef]
24. Gruene, P.; Belova, A.G.; Yegulalp, T.M.; Farrauto, R.J.; Castaldi, M.J. Dispersed Calcium Oxide as a Reversible and Efficient CO_2—Sorbent at Intermediate Temperatures. *Ind. Eng. Chem. Res.* **2011**, *50*, 4042–4049. [CrossRef]
25. Wang, S.; Yan, S.; Ma, X.; Gong, J. Recent advances in capture of carbon dioxide using alkali-metal-based oxides. *Energy Environ. Sci.* **2011**, *4*, 3805–3819. [CrossRef]
26. Tsuneto, A.; Kudo, A.; Saito, N.; Sakata, T. Hydrogenation of solid state carbonates. *Chem. Lett.* **1992**, *21*, 831–834. [CrossRef]
27. Yoshida, N.; Hattori, T.; Komai, E.; Wada, T. Methane formation by metal-catalyzed hydrogenation of solid calcium carbonate. *Catal. Lett.* **1999**, *58*, 119–122. [CrossRef]
28. Proton OnSite Awarded 13 Megawatt Electrolyzers. Available online: https://www.linkedin.com/pulse/proton-onsite-awarded-13-megawatt-electrolyzers-kathleen-mullins (accessed on 20 December 2016).
29. Duyar, M.S.; Treviño, M.A.A.; Farrauto, R.J. Dual function materials for CO_2 capture and conversion using renewable H2. *Appl. Catal. B Environ.* **2015**, *168*, 370–376. [CrossRef]
30. Duyar, M.S.; Wang, S.; Arellano-Treviño, M.A.; Farrauto, R.J. CO_2 utilization with a novel dual function material (DFM) for capture and catalytic conversion to synthetic natural gas: An update. *J. CO_2 Util.* **2016**, *15*, 65–71. [CrossRef]
31. Zheng, Q.; Farrauto, R.; Chau Nguyen, A. Adsorption and Methanation of Flue Gas CO_2 with Dual Functional Catalytic Materials: A Parametric Study. *Ind. Eng. Chem. Res.* **2016**, *55*, 6768–6776. [CrossRef]
32. Bartholomew, C.H.; Farrauto, R.J. Chemistry of nickel-alumina catalysts. *J. Catal.* **1976**, *45*, 41–53. [CrossRef]
33. Kato, T.; Usami, T.; Tsukada, T.; Shibata, Y.; Kodama, T. Study on volatilization mechanism of ruthenium tetroxide from nitrosyl ruthenium nitrate by using mass spectrometer. *J. Nucl. Mater.* **2016**, *479*, 123–129. [CrossRef]
34. Sawada, K.; Ueda, Y.; Enokida, Y. Ruthenium Release from Thermally Overheated Nitric Acid Solution Containing Ruthenium Nitrosyl Nitrate and Sodium Nitrate to Solidify. *Procedia Chem.* **2016**, *21*, 82–86. [CrossRef]
35. Islam, A.; Ravindra, P. *Biodiesel Production with Green Technologies*; Springer International Publishing Switzerland: Cham, Switzerland, 2017; Chapter 1.
36. Batholomew, C.; Farrauto, R.J. *Fundamentals of Industrial Catalytic Processes*; Wiley and Sons: New York, NY, USA, 2006; Chapter 10.
37. Batholomew, C.; Farrauto, R.J. *Fundamentals of Industrial Catalytic Processes*; Wiley and Sons: New York, NY, USA, 2006; Chapter 2; p. 81.